

**KERNFORSCHUNGSZENTRUM  
KARLSRUHE**

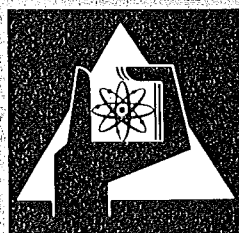
April 1974

KFK 1971

Abteilung Strahlenschutz und Sicherheit

**Nuclear Accident Dosimetry Measurements at the Third  
IAEA Intercomparison, Vinča, Yugoslavia, May 1973**

E. Piesch, B. Burgkhardt



**GESELLSCHAFT  
FÜR  
KERNFORSCHUNG M.B.H.**

**KARLSRUHE**

Als Manuskript vervielfältigt

Für diesen Bericht behalten wir uns alle Rechte vor

GESELLSCHAFT FÜR KERNFORSCHUNG M. B. H.  
KARLSRUHE

KERNFORSCHUNGSZENTRUM KARLSRUHE

KFK 1971

Abteilung Strahlenschutz und Sicherheit

NUCLEAR ACCIDENT DOSIMETRY MEASUREMENTS AT THE THIRD  
I.A.E.A. INTERCOMPARISON VINČA, YUGOSLAVIA, MAY 1973

E. Piesch and B. Burgkhardt

Gesellschaft für Kernforschung, Karlsruhe



## Abstract

The Karlsruhe Nuclear Research Center participated in an international intercomparison of nuclear accident dosimetry systems at Vinča, Yugoslavia, organized by the I.A.E.A.. Results are presented of dosimeter systems exposed to the radiation of the heavy water moderated reactor. Dose estimations for free air and phantom irradiations are based on the results of threshold and activation detectors as well as on the activation of the phosphate glass gamma dosimeter routinely used at Karlsruhe.

In additional experiments the dosimetry properties of albedo neutron dosimeters and of a dosimeter belt of polycarbonate were investigated as well as the neutron response of various solid state gamma dosimeters. The dependence of the detector reading on the direction of the radiation incidence on the surface of a man phantom was studied with threshold detectors, activation detectors and albedo dosimeters.

## Zusammenfassung

Das Karlsruher Kernforschungszentrum nahm an einem von der I.A.E.A. organisierten internationalen Vergleich von Unfalldosimetersystemen in Vinča, Jugoslawien, teil. Es werden die Ergebnisse der Bestrahlungen von Dosimetersystemen am schwerwassermoderierten Reaktor mitgeteilt. Die Dosisabschätzungen für Freiluft- und Phantombestrahlungen basieren auf den Meßergebnissen von Schwellwert- und Aktivierungsdetektoren sowie auf der Aktivierung des in Karlsruhe routinemäßig eingesetzten Phosphatglas-Gammadosimeters.

In zusätzlichen Versuchen wurden die dosimetrischen Eigenschaften eines Neutronen-Albedodosimeters und eines Dosimetergürtels aus Polycarbonat bestimmt sowie die Neutronenempfindlichkeit von verschiedenen Festkörper-Gammadosimetern ermittelt. Die Abhängigkeit der Detektoranzeige von der Richtung des Strahleneinfalls an einem Menschphantom wurde mit Schwellwertdetektoren, Aktivierungsdetektoren und Albedodosimetern untersucht.

NUCLEAR ACCIDENT DOSIMETRY MEASUREMENTS AT THE THIRD  
I.A.E.A. INTERCOMPARISON VINČA, YUGOSLAVIA, MAY 1973

E. PIESCH AND B. BURGHARDT

MARCH 1974

KFK - 1971

1. Introduction
2. Irradiations
3. Description of NAD System
  - 3.1 Routine Dosimeter
  - 3.2 Experimental Detector
  - 3.3 Gamma Dosimeter
4. Measurement Procedures
5. Method of Evaluation
6. Results
  - 6.1 NAD System
  - 6.2 Gamma Dosimeter Study
  - 6.3 Studies with Albedo Neutron Dosimeters
  - 6.4 Phantom Studies with Neutron Detectors
7. References

## List of figures

- Fig. 1 The phosphate glass dosimeter in the spherical capsule and the combination of activation detectors in the routinely used personnel dosimeter at the Karlsruhe Nuclear Research Center
- Fig. 2 Energy dependence of the gamma dosimeter response for the phosphate glass dosimeter, for the TLD-100 and the TLD-200 dosimeter
- Fig. 3 The count rate of Cerenkov light of the Toshiba FD-1 glass as a function of the time after exposure at the Vinča reactor for run No. 2. The total count rate is given by the sum of the  $^{31}\text{Si}$  ( $T_H = 2.6$  h) and  $^{32}\text{P}$  ( $T_H = 14.3$  h) activation fractions.
- Fig. 4 Neutron Energy histogram at the free air stations in front of the Vinča reactor
- Fig. 5 The relative gamma dosimeter reading for free air and phantom exposures measured with phosphate glass and thermoluminescence dosimeters in different capsules
- Fig. 6 The gamma equivalent dosimeter reading for the neutron dose equivalent of 1 rem measured with the Harvey and the Karlsruhe Albedo Dosimeter, respectively, on the front of the phantom in the radiation field of a  $^{252}\text{Cf}$  neutron source and the Vinča reactor
- (1) unshielded source,
  - (2) behind 5 cm Fe,
  - (3) 5 cm PVC,
  - (4) with a high amount of scattered neutrons
  - (5) run no. 1
  - (6) run no. 2

- Fig. 7 Directional dependence of the neutron dose reading of the albedo dosimeter on the surface of a bottle phantom for the Vinča neutron spectrum
- Fig. 8 Directional dependence of the gamma dose reading of the albedo dosimeter on the surface of a bottle phantom
- Fig. 9 Directional dependence of the neutron fluence measured with gold activation and  $^{232}\text{Th}$  threshold detectors at the surface of a bottle phantom for the Vinča neutron spectrum
- Fig. 10 The relative number of recoil tracks measured with a Makrofol E belt on the surface of a bottle phantom as a function of the direction of the radiation incidence for the Vinča neutron spectrum
- Fig. 11 Directional dependence of the albedo neutron dosimeter, of the  $^{232}\text{Th}$  fission fragment detector and of the Makrofol recoil track detector found for the Vinča neutron spectrum on the surface of bottle phantoms of various diameters
- Fig. 12 Directional dependence of the albedo neutron dosimeter and the Makrofol recoil track detector at the Vinča reactor

## List of tables

Tab. 1	Neutron Detectors
Tab. 2	Neutron Fluence-Dose Conversion Factors
Tab. 3	Fluence Dose Conversion Factors
Tab. 4	Number of Activated Atoms or Fission Events for $10^{10}$ Atoms in Free Air
Tab. 5	Fluence Estimates for Activation Detectors
Tab. 6	Fluence Estimates for Threshold Detectors
Tab. 7	Dose Assessments for the Personnel Criticality Dosimeter and the Phosphate Glass Dosimeter
Tab. 8	Dose Estimates for Personnel Dosimeter System exposed in Free Air
Tab. 9	Results of the Personnel Dosimeter for the Phantom Irradiation
Tab. 10	Kerma Estimation for the Free Air Station
Tab. 11	Dose Estimation for Free Air Station
Tab. 12	Comparison of CEA and GfK Dose Results
Tab. 13	Comparison of CEA and GfK Fluence Results
Tab. 14	Gamma Dose Estimates for Phosphate Glass Dosimeter and TLD-700
Tab. 15	Comparison of Gamma Dosimeter Readings for different RPL and RTL Dosimeter
Tab. 16	Bottle Phantom Size for the Albedo Dosimeter Study
Tab. 17	Estimation for Fluence and Dose equivalent for the Bottle Phantom Stations
Tab. 18	Estimation for Kerma and Absorbed Dose for the Bottle Phantom Stations
Tab. 19	Dose Estimation for the Harvey and the Karlsruhe Albedo Dosimeter

Tab. 20 Directional Dependence of Fluence Results for the  
Bottle Phantom Stations

Tab. 21 Dose Estimates and Albedo Dosimeter response for  
the Bottle Phantom Stations

## 1. Introduction

After the First International Intercomparison on Nuclear Accident Dosimetry Systems taking place at the French Atomic Energy Center at Valduc in 1970 [1] and the Second Intercomparison Experiment [2] at the Health Physics Research Reactor of O.R.N.L., Oak Ridge, USA, in 1971 the I.A.E.A. organized a third experiment at the heavy water reactor of the Boris Kidrič Institute at Vinča, Yugoslavia. The intercomparison experiment included the exposure of NAD systems (Nuclear Accident Dosimeter) to radiation from the unshielded, heavy water moderated reactor in area stations and phantom positions, the simultaneous measurement of the detectors immediately after the exposure, a dose assessment for each exposure position and a comparison of the preliminary results indicated by the participants at the end of the meeting. The I.A.E.A. coordinates the collection of the data for comparison of all results as well as work on the collection and unification of neutron leakage spectra from critical assemblies.

The Karlsruhe Nuclear Research Center participated in the international intercomparison experiment in Vinča with the routine personnel dosimeter and with experimental detectors. The experiment at Vinča described here gave us the opportunity to expose the Karlsruhe dosimeter system to a heavy moderated neutron fission spectrum and to calibrate recently developed albedo neutron dosimeters. During the experiment we also investigated the neutron sensitivity of various gamma dosimeters, in particular of phosphate glasses and thermoluminescence dosimeters, which have been used in routine personnel monitoring and in NAD systems, respectively. The neutron fluence spectra were estimated at the area stations and at the phantom surface by using the results of activation and threshold detectors. These data were used to estimate the kerma and the surface absorbed dose. For the albedo dosimeter study the dose equivalent was calculated from the fluence-energy distribution and fluence-dose equivalent conversion factors.

This report describes the NAD system of the Karlsruhe Nuclear Research Center and summarizes the final results of the Karlsruhe measurements. At the time of writing the results of the other participants were not yet available, so that only a comparison was possible of own results with the preliminary results of the participants.

## 2. Irradiations

The irradiation in Vinča takes place at the heavy water RB-reactor. This reactor facility consists of a cylindrical container filled with heavy water, which serves as a reactor core with the fuel elements positioned on the periphery. For the Vinča experiment no shielding was used between the reactor and the exposure positions. Before irradiation the detectors were fastened on plastic foils and then positioned in front of the reactor by the staff of the Boris Kidrič Institute. During the first exposure run the NAD systems were exposed at area stations and on bottle-phantoms, filled with an  $\text{Na}_2\text{CO}_3$ -water solution, concentration  $1.5 \text{ mg Na/cm}^3$ . During the second run they were exposed at area stations and on two Bomab-phantoms. The distance for all area and phantom stations was equal to 3 m in front of the reactor surface and 4.2 m from the reactor center.

The first run took place on May 16th, the reactor was operating at 1.5 kW, during a period of 30 min with 590 Wh total, the second run on May 19th, the reactor was operating at 6 kW, during a period of 25 min with 2600 Wh in total. It was known from preliminary experiments performed at Vinča that the inhomogeneity of the neutron radiation field was lower than  $\pm 20 \%$  at distances of more than 2 m and  $\pm 10 \%$  at distances of more than 3 m with a cadmium ratio of about  $5 \pm 10 \%$ .



Fig. 1: The Personnel Dosimeter used at the Karlsruhe Nuclear Research Center

Table 1 : Neutron Detectors

DETECTOR	DIMENSIONS (mm)	WEIGHT (g)	REACTION	ISOTOPE	HALFLIVE
Sulphur	∅ 12 x 2.4	0.5	n,p	<sup>32</sup> P	14.3 d
Gold	∅ 10 x 0.05	0.073	n,γ	<sup>198</sup> Au	2.7 d
Indium	∅ 10 x 0.25	0.14	n,n	<sup>115m</sup> In	4.5 h
Copper	∅ 10 x 0.12	0.085	n,γ	<sup>64</sup> Cu	12.8 h
Phosphate glass	8 x 8 x 4.7	0.77	n,p	<sup>31</sup> Si	2.6 h
			n,γ	<sup>32</sup> P	14.3 d
Arsenic glass	∅ 10 x 1	0.25	n,γ	<sup>76</sup> As	26.4 h
<sup>237</sup> Np	} 40 μg/cm <sup>2</sup> on steel platelets of ∅ 12		n,f		
<sup>232</sup> Th			n,f		
<sup>238</sup> U			n,f		
Makrofol E	∅ 10 x 0.3		recoils (n,α)		

Table 2 : Neutron Fluence-Dose Conversion Factors

ENERGY RANGE	KERMA herg·g <sup>-1</sup> per n/cm <sup>2</sup>	SURFACE ABSORBED DOSE rd per n/cm <sup>2</sup>
THERMAL NEUTRONS < 0.4 eV	2 x 10 <sup>-11</sup>	6.3 x 10 <sup>-11</sup>
INTERMEDIATE NEUTRONS 1/E SPECTRUM 0.4 eV - 0.75 MeV	2.56 x 10 <sup>-10</sup>	3.56 x 10 <sup>-10</sup>
FAST NEUTRONS UNCOLLIDED FISSION SPECTRUM > 0.75 MeV	3.0 x 10 <sup>-9</sup>	3.62 x 10 <sup>-9</sup>

Tab. 3 : Fluence Dose Conversion Factors

ENERGY RANGE	KERMA herg·g <sup>-1</sup> ·cm <sup>2</sup>	SURFACE ABSORBED DOSE		MULTI COLLISION DOSE rd·cm <sup>2</sup>	Q	DOSE EQUIVALENT rem·cm <sup>2</sup>
		RECOILS + PROTONS rd·cm <sup>2</sup>	H(n,γ) rd·cm <sup>2</sup>			
n <sub>th</sub>	0.2·10 <sup>-10</sup>	0.63·10 <sup>-10</sup>	4·10 <sup>-10</sup>	4.63·10 <sup>-10</sup>	2.3	10.6·10 <sup>-10</sup>
0.4 eV-0.7 MeV	2.56·10 <sup>-10</sup>	3.56·10 <sup>-10</sup>	3·10 <sup>-10</sup>	6.56·10 <sup>-10</sup>	4	26.2·10 <sup>-10</sup>
0.7 - 1.2 MeV	24·10 <sup>-10</sup>	28.8·10 <sup>-10</sup>	1.7·10 <sup>-10</sup>	30.5·10 <sup>-10</sup>	10.5	320·10 <sup>-10</sup>
1.2 - 2.5 MeV	30·10 <sup>-10</sup>	36·10 <sup>-10</sup>	1.5·10 <sup>-10</sup>	37.5·10 <sup>-10</sup>	9.5	355·10 <sup>-10</sup>
2.5 - 10 MeV	38·10 <sup>-10</sup>	46·10 <sup>-10</sup>	1.8·10 <sup>-10</sup>	47.8·10 <sup>-10</sup>	8	382·10 <sup>-10</sup>

### 3. Description of NAD System

#### 3.1 Routine Dosimeter

The Karlsruhe Nuclear Research Center participated in the inter-comparison study with the routine personnel dosimeter as well as with experimental detectors. Our routinely used personnel dosimeter - worn by all people and used as installed dosimeter at the Center - consists of a phosphate glass dosimeter in a spherical capsule and of a combination of activation detectors in an additional plastic badge [1] (Fig. 1 and Tab.1).

The activation detectors in the plastic badge are a sulphur pellet, a bare gold foil, a gold foil covered by indium foils inside a cadmium shielding, a cadmium covered copper foil, an experimental arsenic glass, and a polycarbonate foil (Makrofol E) as a nuclear track detector. The phosphate glass  $\gamma$ -dosimeter is also used as a neutron activation detector for the detection of fast neutrons above a threshold of 2.5 MeV via the reaction  $^{31}\text{P} (n,p) ^{31}\text{Si}$  and for the detection of intermediate neutrons via the reaction  $^{31}\text{P} (n,\gamma) ^{32}\text{P}$  [3].

#### 3.2 Experimental Detector

The experimentally used threshold detector locket consists of neptunium, thorium and uranium detectors which were electroplated in oxide layers of about  $40 \mu\text{g}/\text{cm}^2$  thickness on steel platelets of 1.2 cm diameter. The detectors are in contact with Makrofol N foils. The threshold energies of 0.75 MeV, 1.2 MeV and 1.5 MeV and 2.5 MeV were taken into account for  $^{237}\text{Np}$ ,  $^{232}\text{Th}$ ,  $^{238}\text{U}$  and  $^{32}\text{S}$ . Polycarbonate foils were also used as threshold detectors to measure neutrons above 1 MeV via recoils and  $(n,\alpha)$  reactions [4]. A plastic belt of Makrofol E was provided around the trunk of the phantom to get supplementary information about the angular distribution of the dose. The bare and cadmium covered arsenic glass serves as an activation detector in the intermediate energy range via the reaction  $^{75}\text{As} (n,\gamma) ^{76}\text{As}$  ( $T_H = 26$  hours) [4].

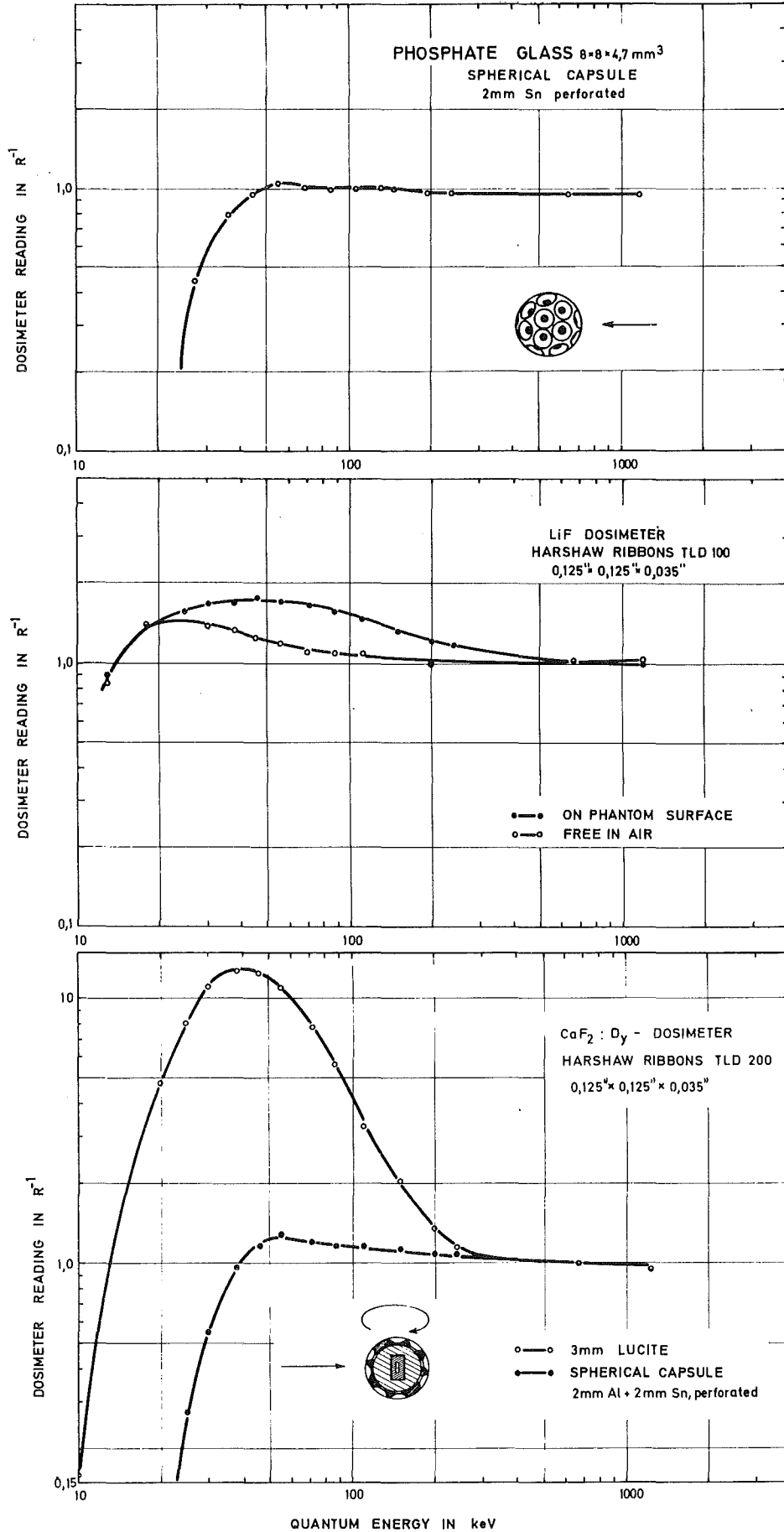


Fig. 2: Energy dependence of the gamma dosimeter response

Intercomparison measurements with an albedo neutron dosimeter [5] were performed to investigate the dosimeter response and the influence of the direction of the radiation incidence under accidental conditions. The albedo dosimeter consists of pairs of LiF dosimeters (Harshaw ribbons of the size  $3 \times 3 \times 0.9 \text{ mm}^3$ ) inside and outside a boron capsule. The neutron dose reading is obtained from the difference in readings between a TLD-600 dosimeter (neutron +  $\gamma$ -dose reading) and a TLD 700 dosimeter ( $\gamma$ -dose reading). In the Vinča experiment the Harvey boron capsule as well as an improved one were used.

### 3.3 Gamma Dosimeter

The routine gamma dosimeter is a phosphate glass of the Toshiba FD-1 type size  $8 \times 8 \times 4.7 \text{ mm}^3$  inside a boron loaded plastic sphere and a perforated tin filter of 2 mm thickness [6]. The dosimeter capsule gives a rem-equivalent indication of  $\gamma$ -radiation and thermal neutrons for the measurement of the exposure in routine personnel monitoring. The determination of neutron fluence by the  $\beta$ -activity of  $^{32}\text{P}$  produced in the glass during neutron capture can be used to correct the respective fraction of the dosimeter reading due to thermal and epithermal neutrons. In addition, new phosphate glasses with low sensitivities to thermal neutrons and thermoluminescence dosimeters of the size  $3 \times 3 \times 0.9 \text{ mm}^3$  (TLD 200, TLD 600, TLD 700 ribbons from Harshaw) were used as experimental detectors (see also 6). For TLD 700 separate corrections of the neutron sensitivity for thermal, intermediate and fast neutrons were used. The energy dependence of the gamma dosimeter reading is given for a free air exposure of the Karlsruhe phosphate glass dosimeter, of TLD-700 and TLD 100 in 4 mm plastic shielding and of TLD 200 in the spherical capsule commonly used for phosphate glasses (Fig.2).

### 4. Measurement Procedures

The  $\beta$ -activity of activation detectors is commonly measured by means of Geiger-Müller counters with a thin window, proportional counters or plastic scintillation counters. For the purpose of

intercomparison studies outside the laboratory it was of interest to measure all kinds of activation detectors with the same measuring equipment. The unification of measurement and calibration result in a simplification and reduction of the measuring procedures and an improvement of the measuring accuracy. During the Vinča experiment no use was made of gamma spectroscopic analysis of the indium and copper detector.

The method of measuring  $\beta$ -activities was standardized for all activation detectors by means of a liquid scintillation counter which seems to be the most favorable equipment with a low background rate of the order of 10 cpm and with a high efficiency and reproducibility for low level measurements. The betas from  $^{31}\text{Si}$ ,  $^{32}\text{P}$  and  $^{76}\text{As}$  can be detected with high efficiency (~ 50 %) and good discrimination against background radiation when using the Cerenkov effect directly induced in the transparent glass by high-energy  $\beta$ -particles above 1 MeV. After exposure the transparent glasses are placed inside the usual plastic bottle liquid scintillation counting in a sample holder made of Lucite, and are measured with the usual channel setting for tritium measurements. The different half-lives of  $^{31}\text{Si}$  (2.6 h) and  $^{32}\text{P}$  (14.3 day) are used to separate the activation fractions in the phosphate glass. The Au-foil and the S-disc are placed between two discs of a plastic scintillator inside the plastic bottle, and are measured with the channel setting for  $^{32}\text{P}$  measurements (efficiency 24 % and 21 %, respectively).

During the intercomparison experiment at Vinča a liquid scintillation spectrometer (Nuclear Chicago Mark I) was used after exposure run No. 1 for  $\beta$ -activity measurements of gold foils, sulphur pellets, arsenic glasses and phosphate glasses. After exposure run No. 2 only an older liquid scintillation counter (Carbotrimètre Liebelin) was available, the reproducibility of which was quite favorable. The sulphur pellets were counted once more in our laboratory because of the low counting rate of the samples and the relatively high background rate of the second

scintillation counter at Vinča. The neptunium results were corrected after the Vinča meeting for the contribution of thermal neutrons. The threshold detector was exposed without a cadmium shielding, the corresponding detection efficiency of our  $^{237}\text{Np}$  detector was found to be 6 % for the thermal fluence.

For the detection of fission fragment tracks in Makrofol the foils were etched for 60 min in a 35 % KOH solution at  $60^{\circ}\text{C}$ , and for the detection of recoils and  $\alpha$ -tracks for 4 hours in the same solution. The nuclear tracks were recorded visually with a microscope or by using a spark counter [4].

The gamma dosimeters are evaluated in a Toshiba phosphate glass reader or in a Harshaw TLD type 2000 A reader. The calibration of the threshold detectors was performed by a standard Am-Be source and a  $^{252}\text{Cf}$  source. Neutron activated calibration detectors in particular Au, S and phosphate glass, are used to transfer the own laboratory counter efficiency to the counter at the laboratory, where the intercomparison takes place.

## 5. Method of Evaluation

Three methods are used to assess the neutron dose:

- From the phosphate glass the neutron induced activity is measured within the first 15 hours ( $^{31}\text{Si}$ ) and 24 hours ( $^{32}\text{P}$ ) after the irradiation.
- From the personnel criticality dosimeter a sulphur disc, a bare and a cadmium shielded gold foil are measured.
- Additional assumptions on the shape of the fission spectrum in the energy range between 0.7 MeV and 10 MeV are based on the results of the threshold detector locket ( $^{237}\text{Np}$ ,  $^{232}\text{Th}$  and  $^{32}\text{S}$ ) exposed at the free air station.

The dose fractions of thermal and intermediate neutrons are determined from the respective fluence values found by the Au-Au/Cd

**Table 4: Number of Activated Atoms or Fission Events for  $10^{10}$  Atoms in Free Air**

DETECTOR	RUN No. 1	RUN No. 2
$^{197}\text{Au}$ bare	$4.63 \times 10^{-2}$	$19.5 \times 10^{-2}$
$^{197}\text{Au}$ in In, Cd	$1.0 \times 10^{-2}$	$5.2 \times 10^{-2}$
$^{32}\text{S}$ bare	$2.09 \times 10^{-6}$	$12.6 \times 10^{-6}$
$^{31}\text{P}$ (n,p) $^{31}\text{Si}$ *	$0.67 \times 10^{-6}$	$4.0 \times 10^{-6}$
$^{31}\text{P}$ (n, $\gamma$ ) $^{32}\text{P}$ *	$4.5 \times 10^{-6}$	$24.6 \times 10^{-6}$
$^{76}\text{As}$ bare	$1.7 \times 10^{-3}$	$9.8 \times 10^{-3}$
$^{237}\text{Np}$ bare	$0.34 \times 10^{-4}$	$2.02 \times 10^{-4}$
$^{232}\text{Th}$ bare	$0.23 \times 10^{-5}$	$1.17 \times 10^{-5}$

\*) Phosphate glass in boron sphere used as routine gamma dosimeter

system or the  $\beta$ -activity of  $^{32}\text{P}$  in the phosphate glass assuming an intermediate  $1/E$  spectrum and a thermal Maxwellian spectrum. The dose fraction of fast neutrons above 0.75 MeV is estimated on the basis of an unmoderated fission spectrum by using the sulphur and phosphorus detectors. For the Vinča spectra no assumption on the shape of the fission spectra was necessary to evaluate the personnel dosimeter. The fluence - kerma conversion factors and the fluence - absorbed dose conversion factors, respectively used for the personnel dosimeter are given in Table 2 [7, 8]

The threshold detectors  $^{237}\text{Np}$ ,  $^{232}\text{Th}$ ,  $^{32}\text{S}$  were evaluated to estimate the neutron fluence in the energy range 0.75 - 1.2 MeV, 1.2 - 2.5 MeV and 2.5 - 10 MeV, respectively. The corresponding fluence-kerma conversion factors in Tab. 3 were used referring to data given by F.F. Haywood for the Oak Ridge threshold detector unit [9]. The fluence-dose equivalent conversion factors are based on the ICRP recommendation and the factors for the surface absorbed dose from heavy charged particles on calculations by Auxier [10].

Tab. 5 : Fluence Estimates for Activation Detectors

NEUTRON FLUENCE IN $10^{10}$ n/cm <sup>2</sup>						
	Au <0.4 eV	Au <sup>1)</sup> >0.4 eV	As <0.4 eV	As <sup>2)</sup> >0.4 eV	As	Phosphate glass In B <sup>3)</sup>
<u>RUN No 1:</u>						
Free air	3.8	2.3	-	-	3.1	2.5
Phantom I front	6.0	2.6	-	-	4.1	3.8
belt front	4.9	2.3	3.5	0.9	4.4	3.6
back	0.71	0.29	0.65	0.1	0.75	0.65
<u>RUN No 2:</u>						
Free air	15.0	12.0	-	-	17.8	13.7
Phantom I front	20.3	13.0	-	-	28.3	20.0
Phantom II front	20.2	13.1	23.6	6.8	30.4	20.0
back	3.4	1.9	4.5	0.8	5.23	2.9

<sup>1)</sup> Au covered by In and Cd

<sup>2)</sup> As in Cd

<sup>3)</sup> Phosphate glass dosimeter (Routine  $\gamma$ -Dosimeter) in spherical capsule inside of a boron loaded plastic sphere

Table 6: Fluence Estimates for Threshold Detectors

	NEUTRON FLUENCE IN $10^{10}$ n·cm <sup>-2</sup>				
	<sup>237</sup> Np > 0.75 MeV	MAKROFOL > 1 MeV	<sup>232</sup> Th > 1.2 MeV	<sup>31</sup> P > 2.5 MeV	<sup>32</sup> S > 2.5 MeV
<u>RUN No 1</u>					
Free air	0.245	0.21	0.18	0.092	0.094
Phantom I front	0.22			0.101	0.103
belt front	0.2			0.101	0.099
<u>RUN No 2</u>					
Free air	1.46	0.98	0.94	0.55	0.56
Phantom I front	1.5			0.57	0.585
Phantom II front	1.3			0.57	0.59

Tab. 7 : Dose Assessments for the Personnel Criticality Dosimeter and the Phosphate Glass Dosimeter

IRRADIATION	- KERMA IN h.erg.g <sup>-1</sup>							
	PERS. CRITICALITY DOSIMETER				PHOSPHATE GLASS DOSIMETER			
	Au <0.4 eV	Au (in Cd,In)	S	NEUTRON TOTAL	<sup>32</sup> P	<sup>31</sup> Si	NEUTRON TOTAL	γ-DOSE rd
<u>RUN No 1:</u>								
Free air	0.76	5.8	8.0	14.6	6.4	7.8	14.2	37
Phantom I front	1.2	6.7	8.8	16.7	9.7	8.5	18.2	55
belt front	0.98	5.9	8.4	15.3	9.2	8.5	17.7	55
back	0.14	0.75						17
<u>RUN No 2:</u>								
Free air	3.0	30.8	48.5	82	35	46.5	81.5	238
Phantom I front	4.1	33.4	50.5	88	51	48.6	100	308
Phantom II front	4.05	33.6	51	88.7	51	48.7	100	316
back	0.68	4.9						125

Tab. 8 : Dose Estimates for Personnel Dosimeter System exposed In Free Air

	FLUENCE IN 10 <sup>10</sup> n.cm <sup>-2</sup>					KERMA h.erg.g <sup>-1</sup>	NEUTRON DOSE* rd	GAMMA DOSE rd
	n <sub>th</sub>	>0.4 eV	>0.75 MeV	>1.2 MeV	>2.5 MeV			
<u>RUN No 1</u>								
Provis. Results	3.8	2.3	0.39	-	0.090	15.8	20.0	40
Person.Critic.Dos.	3.8	2.55	0.245	0.18	0.094	14.2	19.3	-
Phosphate Glass	-	2.5	--	-	0.092	14.2	-	37
<u>RUN No 2</u>								
Prov. Results	15.0	13.8	1.7	-	0.50	89	107	235
Person.Critic.Dos.	15.0	13.5	1.46	0.94	0.56	79.2	105	-
Phosphate Glass	-	13.7	-	-	0.55	81.5	-	238

\* ) Assumed dose at area location

## 6. Results

### 6.1 Nuclear Accident Dosimeter System

For an intercomparison and interpretation of the neutron detector results with that of other participants the measured activities and fission rates were converted into reaction rates. Table 4 shows the number of activated atoms or fission events for  $10^{10}$  atoms for each of the detector exposed in free air.

The results of fluence estimation are given in Table 5 for the activation detectors gold, arsenic, phosphate glass in the boron loaded capsule and in Tab.6 for the threshold detectors  $^{237}\text{Np}$ , Makrofol,  $^{232}\text{Th}$ ,  $^{31}\text{P}$  and  $^{32}\text{S}$ . Starting from the fluence results the neutron doses have been estimated by using fluence-dose conversion factors from Table 2. The kerma values at the free air station were calculated from the neutron energy spectrum found with the threshold detectors at the same location. The final results for the free air station in Table 8 are based on the threshold detector measurements as opposed to the provisional results providing the dose estimation only based on sulphur. The reduction of the  $^{237}\text{Np}$  data can be explained by a correction for thermal neutrons, because that detector was not exposed in a cadmium capsule. At the phantom stations (Table 7) for fast neutrons only the sulphur and the phosphorus results, respectively were transferred to kerma taking into account fluence-kerma conversion factors for a fission spectrum. In this case no correction was made using results of the neutron spectrum at the free air station. The gold foil and sulphur activities were used in the standard way to give the dose fractions of thermal, intermediate and fast neutrons. A similar evaluation was used for the two activation reactions in the phosphate glass dosimeter.

The phantom kerma results of the phosphate glass seem to be higher by about 10 % compared to the results of the personnel criticality dosimeter due to the different cross sections in the energy range of intermediate neutrons.

Tab. 9 : Results of the Personnel Dosimeter for the Phantom Irradiation

	KERMA $\text{h}\cdot\text{erg}\cdot\text{g}^{-1}$	NEUTRON DOSE (rd)		GAMMA DOSE (rd)
		RECOILS	H(n, $\gamma$ )	
RUN No 1:				
Prov. Results:GFK	15.5	21.4		46
Mean Value <sup>1)</sup> )	15.7	22.1	32	49.5
Final results GFK	15.3	21.3		55
RUN No 2:				
Prov. Results GFK	86.4	117		280
Mean value <sup>1)</sup> )	86.4	117	129	306
Final results GFK	88	119.9		308

<sup>1)</sup> Prov. results from all participants calculated during the Vinča meeting

Tab. 10: Kerma Estimation for the Free Air Station

ENERGY RANGE	FLUENCE $10^{10}\text{n}\cdot\text{cm}^{-2}$		KERMA $\text{h}\cdot\text{erg}\cdot\text{g}^{-1}$	
	RUN 1	RUN 2	RUN 1	RUN 2
0.01-0.4 eV	3.8	15.0	0.76	3
0.4 eV - 0.75 MeV	2.3	12.0	5.8	30.8
0.75 - 1.2 MeV	0.065	0.52	1.55	12.5
1.2 - 2.5 MeV	0.087	0.38	2.6	11.4
2.5 - 10 MeV	0.093	0.56	3.5	21.5
0.75 - 10 MeV	0.245	1.46	7.65	45.4
0.01 eV - 10 MeV	6.345	28.46	14.21	79.2

The neutron induced  $\beta$ -activity measured in the phosphate glass dosimeter is presented in Fig.3 as a function of the elapsed time after the end of run No.2. Two measurements are necessary for the separation of  $^{31}\text{S}$  and  $^{32}\text{P}$ . The final results found for the phantom irradiation with gold and sulphur detectors are presented in Table 9. Here a comparison can be made between the mean value of results presented by all participants at the end of the Vinča meeting and our preliminary results as well as our final results. The neutron dose given in this table is the absorbed dose at the front surface of the phantom. The gamma dose measured with the phosphate glass is the total surface absorbed dose due to incident gamma rays and that produced by the  $^1\text{H}(n,\gamma)^2\text{D}$  reaction in the phantom. The provisional gamma results were found with the RPL-V glass on the water bottle phantom (see also Table 15).

The neutron energy spectra at the Vinča reactor were estimated for the free air station from the results of activation and threshold detectors and are shown in Table 10 for the neutron fluence and the kerma.

Tab. 11: Dose Estimation for Free Air Station

	FLUENCE $10^{10} \text{ ncm}^{-2}$	KERMA $\text{herg}\cdot\text{g}^{-1}$	ABSORBED DOSE RECOILS rd	DOSE EQUIVALENT rem	
				RECOILS	MC
<u>RUN 1</u>					
$n_{th}$	3.8	0.76	2.4	5.5	40.3
$n_i$	2.3	5.9	8.2	32.8	60.2
0.75 - 1.2 MeV	0.065	1.56	1.87	19.6	20.8
1.2 - 2.5	0.09	2.70	3.24	30.8	32
2.5 - 10	0.093	3.54	4.3	34.4	35.5
	6.348	14.46	20.0	123.1	189.8
<u>RUN 2</u>					
$n_{th}$	15	3	9.4	21.6	159
$n_i$	12	30.8	42.7	171	314
0.75 - 1.2 MeV	0.52	12.5	15.0	158	166
1.2 - 2.5	0.38	11.4	13.8	131	135
2.5 - 10	0.56	21.3	25.8	206	214
	28.46	79.0	107	687.6	988

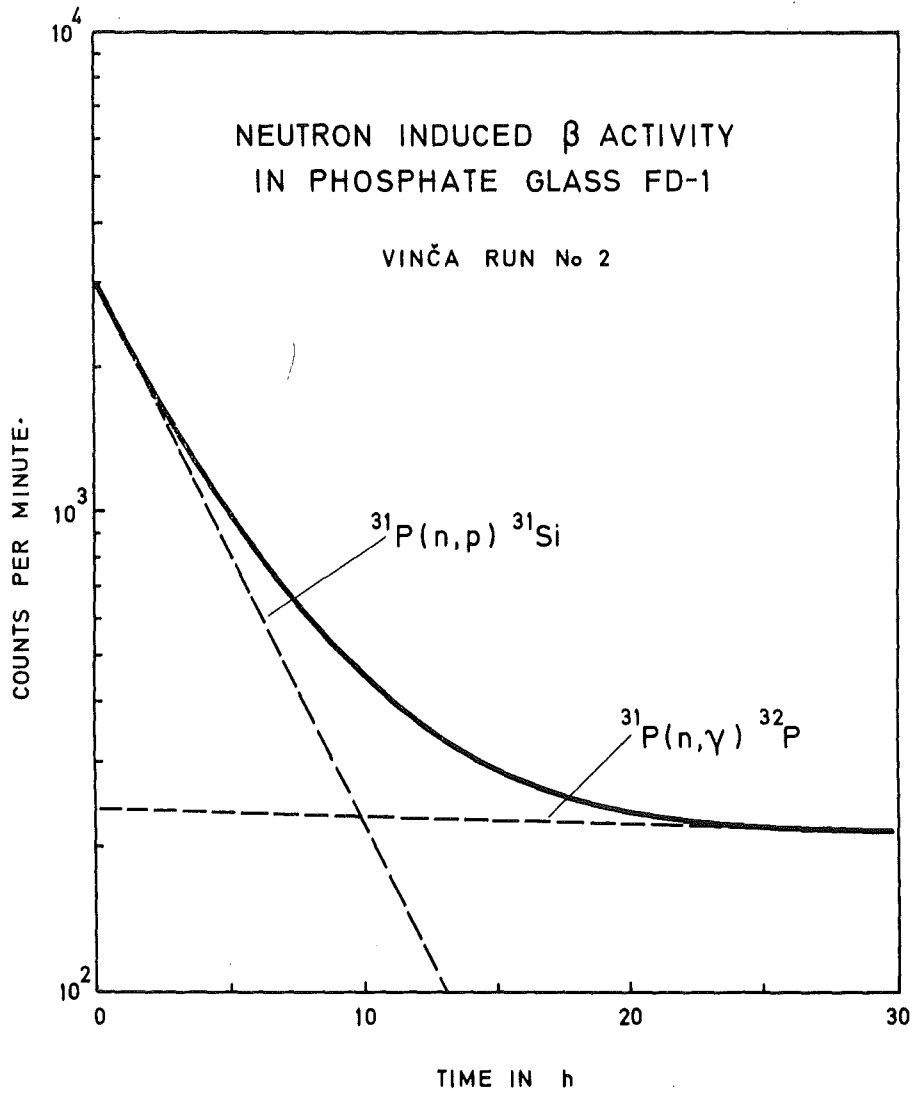


Fig. 3: The count rate of Cerenkov light of the Toshiba FD-1 glass as a function of the time after exposure at the Vinča reactor for run no. 2. The total count rate is given by the sum of the  $^{31}\text{Si}$  ( $T_H = 2.6$  h) and  $^{32}\text{P}$  ( $T_H = 14.3$  h) activation fractions.

Tab. 12: Comparison of CEA and GfK Dose Results

	DOSIMETER READING		
	CEA	GfK	$\frac{\text{GfK}}{\text{CEA}}$
<u>RUN 1 Free air</u>			
fluence $10^{10} \text{n}\cdot\text{cm}^{-2}$	6.44	6.35	0.99
kerma $\text{herg}\cdot\text{g}^{-1}$	13.1	14.5	1.11
abs. dose rd	17.1	20	1.77
dose equivalent rem	205	190	0.93
<u>RUN 1 Bottle Phantom</u>			
fluence $10^{10} \text{n}\cdot\text{cm}^{-2}$	7.57	8.28	1.1
kerma $\text{herg}\cdot\text{g}^{-1}$	10.4	13.3	1.28
dose equivalent rem	187	175.5	0.94
<u>RUN 2 Free air</u>			
fluence $10^{10} \text{n}\cdot\text{cm}^{-2}$	38.7	28.46	0.74
kerma $\text{herg}\cdot\text{g}^{-1}$	95.5	79	0.83
abs. dose rd	115	107	0.93
dose equivalent rem	1420	988	0.69

Tab. 13: Comparison of CEA and GfK Fluence Results

	FLUENCE READING #)		
	CEA	GfK	$\frac{\text{GfK}}{\text{CEA}}$
<u>RUN 1 Free air</u>			
$n_{\text{th}}$	3.72	3.8	1.02
$n_{\text{i}}$	2.43	2.3	0.95
> 0.7 MeV	0.29	0.25	0.86
$n_{\text{th}} - 10 \text{ MeV}$	6.44	6.35	0.99
<u>RUN 1 Bottle Phantom</u>			
$n_{\text{th}} - 10 \text{ MeV}$	7.57	8.28	1.1
<u>RUN 2 Free air</u>			
$n_{\text{th}}$	21.7	15	0.69
$n_{\text{i}}$	15.4	12	0.78
> 0.7	1.8	1.5	0.83
$n_{\text{th}} - 10 \text{ MeV}$	38.7	28.5	0.74

#) in  $10^{10} \text{n}\cdot\text{cm}^{-2}$

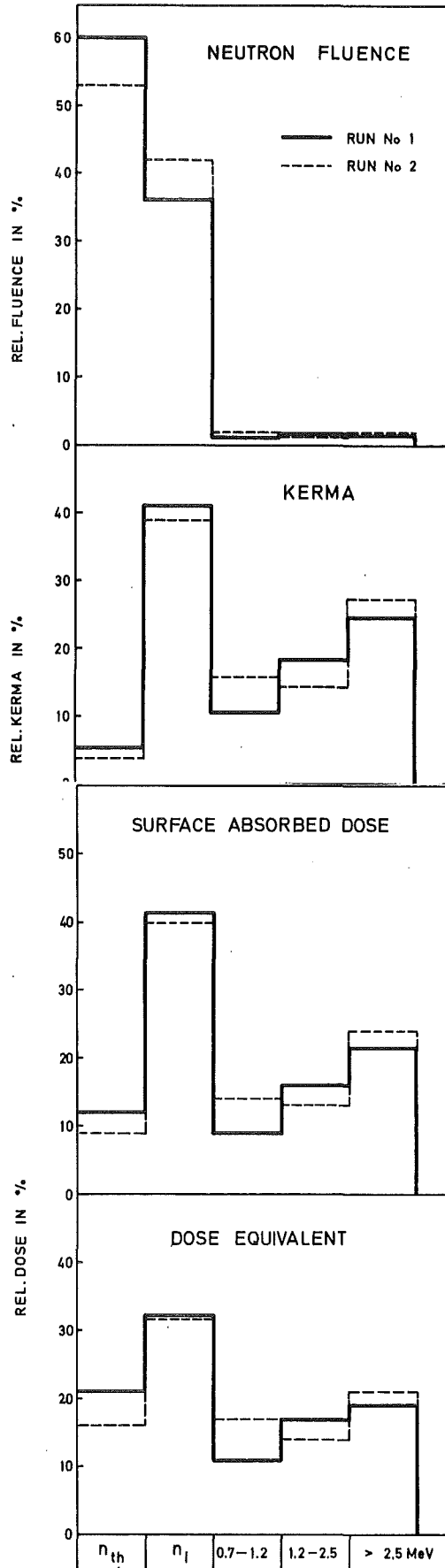


Fig. 4: Neutron Energy Histogram at the Vinča Reactor

For the albedo neutron dosimeter study it was necessary to calculate the surface absorbed dose and the dose equivalent for the exposure positions on the reactor site. The calculation was performed with fluence-dose conversion factors presented in Table 3. Table 11 shows the estimated data at the area station for kerma, surface absorbed dose from heavy charged particles and from the  $H(n,\gamma)D$  reaction as well as the dose equivalent from the surface absorbed dose and the ICRP recommendation, respectively.

The energy histogram (Fig.4) of the neutron fluence at the area station shows that more than 95 % of the neutrons are in the energy range below 0.7 MeV. Looking for the kerma corresponding or the dose equivalent distribution the dose fraction of intermediate neutrons was found to be of the order of 40 % and 32 %, respectively, the dose fraction of thermal neutrons 5 % and 20 %, respectively.

The Vinča neutron spectra were also calculated for the area stations as well as for the bottle-phantom 1 of the albedo dosimeter experiment based on the experimental results of the SNAC 50 neutron spectrometer. This French NAD system consists of a set of activation detectors which allows to determine unknown neutron spectra by a linear combination of "model spectra" [11]. In connection with the SNAC 003 computer code the neutron spectra and for every energy range the fluence, the kerma or the dose equivalent can be indicated. The results for fluence, kerma, and dose equivalent measured with the SNAC spectrometer [12] and with our threshold detectors are presented in tables 12 and 13. A difference in the results should be expected due to the different measuring methods-particularly in the energy range of intermediate neutrons, where the gold activation is calibrated for a  $1/E$  spectrum - and due to different calculation methods and fluence-dose conversion factors. The agreement of the dose equivalent results was found to be better than 7 % for run no. 1 at the area station as well as for run no. 2 on the bottle phantom of the albedo-dosimeter experiment (see 6.3).

Here both dosimeter systems were exposed nearly at the same position. This was not the case for run No. 2 where the field inhomogeneity was found to be of the order of 30 % for the dose equivalent as well as for the neutron fluence results in particular for thermal neutrons.

These results show a significant change of the neutron fluence spectra dependent on the exposure positions for both the area station and the bottle 1 phantom station of run No. 1 but also field inhomogeneities between the two exposure positions (CEA, GfK) run No. 2.

### 6.2 Gamma Dosimeter Study

An accurate measurement of the gamma exposure in case of a nuclear accident can be made only by means of suitable gamma dosimeters whose neutron sensitivities are low or known for a correction of the dosimeter reading. It is therefore of interest to calibrate the gamma dosimeters with thermal neutrons and with various kinds of neutron accident spectra.

Tab. 14 : Gamma Dose Estimates for Phosphate Glass Dosimeter and TLD-700

	$\gamma$ -Dosimeter Reading (rd).						
	GLASS FD-1			TLD-700			
	measured	Correction	Corrected	measured	Correction $n_{th}$	Correction $n_1$	Corrected
<u>RUN No 1</u>							
Free air	61	24	37	46	5.0	2.9	38.1
Phantom I front	92	36.6	55.4	69.3	7.8	3.3	58.2
belt front	90	34.6	55.4	65.1	6.4	2.9	55.8
back	23.5	6.2	17.3	17.9	0.9	0.4	16.6
<u>RUN No 2</u>							
Free air	370	132	238	278	19.5	15	243.5
Phantom I front	500	192	308	409	26.4	16.3	366.3
Phantom II front	508	192	316	407	26.2	16.4	364.4
back	153	28	125	157	4.4	2.4	150.2

At the Karlsruhe Nuclear Research Center the phosphate glass of the Toshiba type FD-1 has been used in a spherical capsule with a boron content to reduce the thermal neutron oversensitivity up to a dose equivalent reading. The neutron correction of the gamma dosimeter reading is directly based on the measurement of phosphorus activation in the glass. For the FD-1 glass a fluence of  $10^{10}$  n/cm<sup>2</sup> gives a gamma equivalent reading of 10 R [1]. Using Harshaw TLD 700 thermoluminescence dosimeters, a correction for thermal, intermediate and fast neutrons was found to be necessary. During the intercomparison experiment at the Dosar Facility at Oak Ridge the correction factor used for TLD 700 was 1.3 rad for thermal neutrons and 1.25 rad for intermediate and fast neutrons per  $10^{10}$  n/cm<sup>2</sup> [2].

The estimation of the gamma dose for the intercomparison study (see results in 6.1) is given in Tab. 14 for the phosphate glass and the LiF dosimeter. After correction of the dosimeter readings both dosimeters show comparable results except for the higher results for TLD 700 at the phantom station of Run 2.

Additional investigations were performed to study the neutron response of various solid state gamma dosimeters which were commonly used in routine personnel monitoring as well as in accident dosimetry. The phosphate glasses size  $8 \times 8 \times 4.7$  mm<sup>3</sup>, which were used in the spherical capsule and in a 1.2 mm thick tin capsule, respectively, were the FD-1 and FD-7 type from Toshiba, the RPL-V type and an experimental glass with an arsenic content from Schott and Gen. The CEC glass was used in the tantalum capsule. Harshaw TLD-700 and TLD-200 ribbons of the size  $3 \times 3 \times 0.9$  mm<sup>3</sup> were uncapsulated in 4 mm thick lucite and TLD-200 also in the spherical dosimeter with a boron content for energy compensation (s. Fig.2) [13]. The dosimeter reading of these dosimeters are presented in Table 15 and for run No. 2 in Fig.5.

Tab. 15 : Comparison of Gamma Dosimeter Readings for different RPL and RTL Dosimeter

	DOSIMETER READING (rd)					
	RUN No 1			RUN No 2		
	FREE AIR	PHANTOM FRONT	PHANTOM BACK	FREE AIR	PHANTOM FRONT	PHANTOM BACK
<b>PHOSPHATE GLASS (IN BORON)</b>						
RPL-V	36.4	40	16.6	220	251	112
FD-1	62.4	75	24	346	432	135
FD-7	44.5	47	19.3	258	274	123
Schott-Exp.	60	81	24	362	485	148
<b>PHOSPHATE GLASS (IN Sn)</b>						
RPL V	39.2	43.6	18.5	251	274	117
FD-7	39.5	44.5	19.9	246	275	128
Schott-Exp.	208	252	73.5	1190	1445	450
<b>PHOSPHATE GLASS (IN TANTAL)</b>						
CEC	269	250	60	1075	1498	332
TLD-700	39.2	50.3	16.7	253	311	106
CaF <sub>2</sub> :Dy	32.5	40.7	15.4	255	344	114
CaF <sub>2</sub> :Dy (BORON)	32	38.4	13.7	236	307	94.8
FD-1 corrected	38.4	40.5	17.7	214	240	107
RPL-V corrected	34.8	37.5	17.7	234	251	113
TLD-700 corrected	32	39.3	15.4	218	268	99

The relative dosimeter reading in Fig. 5 is based on the results of the RPL-V glass which shows low neutron sensitivity. Different components or activators in the solid state detectors but also recoil nuclei are responsible for the neutron sensitivity which can be reduced to a small extent by using neutron absorbers as shielding materials. It can be seen from this Fig. that neutron moderation and backscatter in the phantom increase the dosimeter

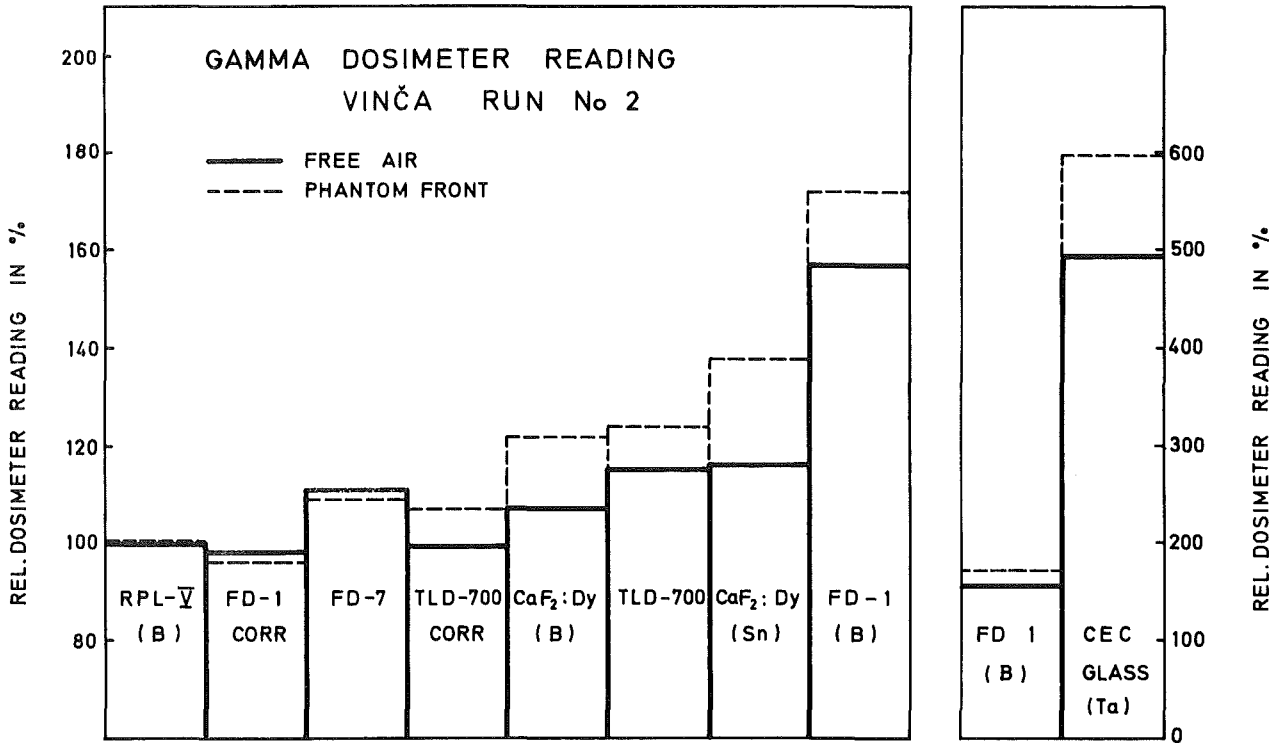


Fig. 5: The relative gamma dosimeter reading for free air and phantom exposures measured with phosphate glass and thermoluminescence dosimeters in different capsules

reading and the overestimation of the gamma exposure can exceed a factor of 2. The neutron sensitivity of gamma dosimeters is naturally a function of the neutron spectrum and will be influenced by activation dosimeters positioned nearby and by the activation effects in the capsule. The gamma dosimeter used for the additional investigations (Tab. 15) were exposed in separate positions, where no activation detectors from other participants had been positioned. Besides this, the water bottles used as phantoms have been filled up without any additional sodium concentration. This is the reason for a higher dosimeter reading with a remarkable contribution of  $^{24}\text{Na}$  gamma rays as shown by the dosimeter results from the remab phantom stations (Tab. 14).

### 6.3 Studies with Albedo Neutron Dosimeters

In 1972 experimental investigations performed at the Karlsruhe Nuclear Research Center with the Harvey albedo neutron dosimeter led to a dosimeter which consists of two pairs of LiF dosimeters one positioned inside and one outside the boron capsule [5]. The ratio of the dosimeter readings  $D_a/D_i$  was used to correct the dosimeter reading  $D_i$  for the contribution of thermal neutrons scattered from the environment. Calibration exposures carried out with  $^{252}\text{Cf}$  fission neutrons and Am-Be neutrons behind various shieldings and in neutron fields with a high amount of back-scattered radiation have shown that the dose equivalent reading of the albedo neutron dosimeter is approximately independent of the neutron energy in the range above 100 keV up to 14 MeV. The neutron response of the albedo dosimeter was referred to the reading of an Anderson-Braun type rem-counter and was found to be 0.54 R/rem expressed as a gamma equivalent reading with a maximum deviation of  $\pm 30\%$  attributed to influences of back-scattering, neutron energy spectrum and different directions of radiation incidence. These extensive intercomparison studies were performed with albedo dosimeters as well as with the Kodak NTA film,  $^{237}\text{Np}$  and  $^{232}\text{Th}$  track etching detectors and have been reported in [14].

Because of its oversensitivity to thermal and intermediate neutrons the albedo neutron dosimeter overestimates the dose equivalent reading up to a factor of 6 particularly on reactor sites. Such unfavorable conditions exist near beamholes of research reactors at positions, where the phantom was enclosed by concrete shieldings at a distance of less than 20 cm.

To improve the dosimeter response the construction of the boron capsule was changed which resulted in an additional dosimeter pair (m) encapsulated in boron. In the intercomparison experiment performed at Vinča both types of albedo dosimeters were calibrated.

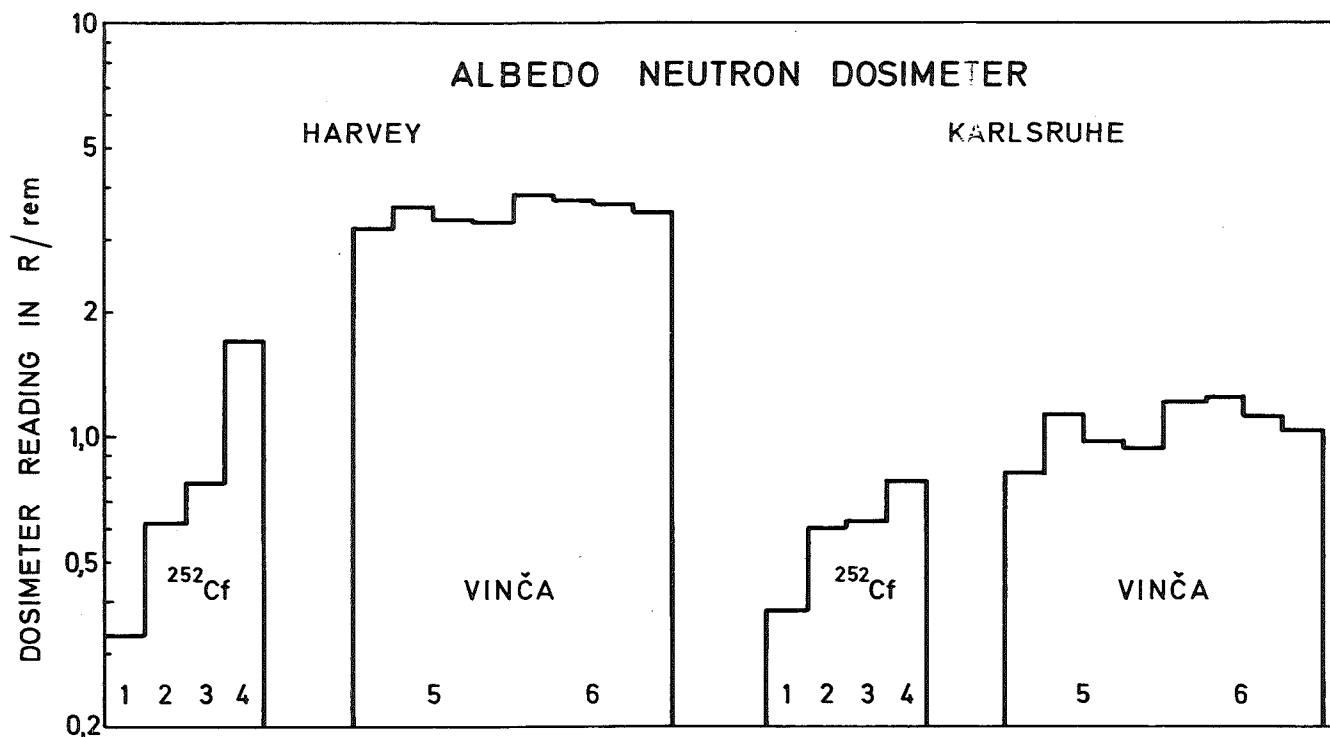


Fig. 6: The gamma equivalent dosimeter reading for the neutron dose equivalent of 1 rem measured with the Harvey and the Karlsruhe albedo dosimeter, respectively, on the front of the phantom in the radiation field of a  $^{252}\text{Cf}$  neutron source and the Vinča reactor

- |                        |                           |
|------------------------|---------------------------|
| (1) unshielded source, | (4) with a high amount of |
| (2) behind 5 cm Fe,    | scattered neutrons        |
| (3) 5 cm PVC           | (5) run no. 1             |
|                        | (6) run no. 2             |

At the Vinča reactor water filled bottles of various sizes were used as phantoms to calibrate the albedo dosimeters (see Table 16). Activation and threshold detectors were exposed on the surface of each bottle at positions at  $0^{\circ}$ ,  $90^{\circ}$  and  $180^{\circ}$

Table 16: Bottle Phantom Size for the Albedo Dosimeter Study

BOTTLE PHANTOM SIZE		
	VOLUME IN l	$\phi$ in cm
Phantom 1	25	28
Phantom 2	10	21
Phantom 3	10	21
Phantom 4	5	16.5

to the direction of the radiation incidence. From these detector readings the fluence-energy histogram was determined relative to a nominal free air exposure at the position of each phantom. The fluence results found for thermal and intermediate neutrons on the phantom were corrected for the phantom influence based on the results of the free air station. The fluence-dose conversion factors presented in Tab. 3 were used in the corresponding neutron energy ranges to calculate the kerma, the surface absorbed dose and the dose equivalent.

For the first evaluation it was assumed that all phantoms had been irradiated in the same radiation field. In this case the dose results found for the free air dosimeter station (Tab. 11) were used as a reference. Based on the results of the free air station the response of the albedo dosimeters are presented in Fig. 6 for the Harvey albedo dosimeter as well as for the Karlsruhe albedo dosimeter irradiated at the front of the phantoms. In this figure the results of phantom irradiations in the neutron field of a  $^{252}\text{Cf}$  source are also shown for an exposure without shielding (1), with a shielding of 5 cm Fe (2) and of 5 cm PVC (3) and with a high amount of backscattered neutrons (4) emitted from a water moderator. For the Vinča spectrum a neutron response of 3.6 R/rem expressed as a gamma equivalent reading was

Table 17: Estimation for Fluence and Dose equivalent for the Bottle Phantom Stations

	FLUENCE $n \cdot \text{cm}^{-2} \cdot 10^{-10}$				DOSE EQUIVALENT rem			
	PH 1	PH 2	PH 3	PH 4	PH 1	PH 2	PH 3	PH 4
<b>RUN 1</b>								
$n_{th}$	3.80	3.7	3.62	3.34	40.2	39	38.3	35.4
$n_m$	2.78	2.56	2.4	2.56	73	67	63	67
$n_{> 1.2 \text{ MeV}}$	0.126	0.186	0.196	0.163	62	91.2	96	80
					175.5	197.4	197.3	182.4
<b>RUN 2</b>								
$n_{th}$	26	25.4	25.4	20.2	276	270	270	214
$n_i$	16.6	16.5	17.2	14.6	435	432	450	382
$n_{> 1.2 \text{ MeV (1)}}$	0.86	1.06	1.02	0.915	471	580	555	500
$n_{> 2.5 \text{ MeV (2)}}$	0.56	0.51	0.6	0.585	515	470	550	540
					1182	1282	1275	1096
					1226	1172	1270	1136

Table 18: Estimation for Kerma and Absorbed Dose for the Bottle Phantom Stations

	KERMA $\text{herg} \cdot \text{g}^{-1}$				SURFACE ABSORBED DOSE (RECOILS + PROTONS) rd			
	PH 1	PH 2	PH 3	PH 4	PH 1	PH 2	PH 3	PH 4
<b>RUN 1</b>								
$n_{th}$	0.76	0.74	0.73	0.67	2.4	2.33	2.28	2.1
$n_i$	7.1	6.55	6.15	6.55	9.9	9.1	8.55	9.1
$n_{> 0.7 \text{ MeV}}$	5.45	8.05	8.5	7.05	6.6	9.7	10.25	8.5
	13.3	15.3	15.4	14.3	18.9	21.1	21.1	19.7
<b>RUN 2</b>								
$n_{th}$	5.2	5.1	5.1	4.1	16.4	16	16	12.7
$n_i$	42.5	42.3	44	37.4	59	59	61	52
$n_{> 0.7 \text{ MeV (1)}}$	41.5	51	49	44	50	61.5	59	53
$n_{> 0.7 \text{ MeV (2)}}$	45.2	41	48.5	47.3	54.6	50	58.5	57
(1)	89.2	98.4	98.1	85.5	125.4	136.5	136.0	117.7
(2)	92.9	88.4	97.6	88.8	130.0	125	135.5	121.7

found for the Harvey dosimeter and about 1 R/rem for the Karlsruhe albedo dosimeter compared with the response of 0.5 R/rem to  $^{252}\text{Cf}$  neutrons.

The evaluation of the neutron detectors on the front side of the phantom gives neutron fluence results and the corresponding neutron doses in tables 17 and 18. The dose fraction of fast neutrons was determined taking into account the results of  $^{232}\text{Th}$  track etching detectors (1) or the results of sulphur threshold detectors (2). The dose equivalent found at the phantom positions differ up to a value of 12 % from that at the free air station. Based on these results the albedo dosimeter response was determined and presented in Tab. 19 for the Harvey albedo dosimeter and the Karlsruhe albedo dosimeter. This table shows data of the LiF dosimeter readings inside (i) and outside (a) the boron capsule as well as the correction factor k corresponding to the ratio a/i.

**Table 19:** Dose Estimation for the Harvey and the Karlsruhe Albedo Dosimeter

ALBEDO-NEUTRON DOSIMETER				
	PHANTOM IRRADIATION			
	1	2	3	4
<b>RUN 1</b>				
i in R	605	687	635	634
a in R	4213	3775	3831	4059
a/i	7.0	5.5	6.0	6.4
k	0.26	0.31	0.29	0.28
i·k in R	157	213	184	178
i·k/D R/rem	0.9	1.08	0.94	0.98
i/D R/rem	3.46	3.54	3.23	3.48
<b>RUN 2</b>				
i in R	3799	3712	3597	3424
a in R	19435	18231	19901	19104
a/i	5.1	4.9	5.5	5.6
k	0.32	0.33	0.31	0.30
i·k in R	1210	1230	1110	1030
i·k/D R/rem	0.99	1.05	0.88	0.91
i/D R/rem	3.1	3.18	2.84	3.0

The dose estimates and the albedo dosimeter response for the bottle phantom stations are presented in Tab. 21.

In the case of frontal irradiation the neutron response of the Karlsruhe albedo dosimeter was found to be about 1 R/rem. The influence of the phantom size on the dosimeter reading is less than 10 %. For the purpose of accident dosimetry the kerma or the surface absorbed dose from heavy charged particles have to be measured. Here the dosimeter response is of the order of 13 R/nerg·g<sup>-1</sup> and 9.7 R/rad, respectively. It should be pointed out that the response of albedo dosimeters depends extremely on the distance of the dosimeter to the body. The albedo dosimeter should therefore be used practically only as a belt dosimeter.

Additional studies were performed to investigate the directional dependence using an experimental capsule with an additional LiF dosimeter pair (m) encapsulated in boron. The dosimeter reading as a function of radiation incidence is given in Fig.7 for the neutron dosimeter reading TLD 600-TLD 700 and in Fig.8 for the gamma dosimeter reading TLD 700. Compared to a front exposure at 0° the dosimeter reading at 180° was found to be 17 % for fast neutrons and 42 % for gamma rays. These results are comparable with those of other detector types. The capture gamma rays which were induced by neutrons in the boron capsule did not influence the gamma dosimeter reading.

The results of the new albedo dosimeter capsule are in good agreement with those found with <sup>252</sup>Cf neutrons on reactor sites and at the HPRR in Oak Ridge. At the unshielded Vinča reactor the response of the albedo neutron dosimeter is still higher by a factor 2 [15]. The investigations with the new capsule will be completed in the near future by additional calibration exposures at various power reactor stations.

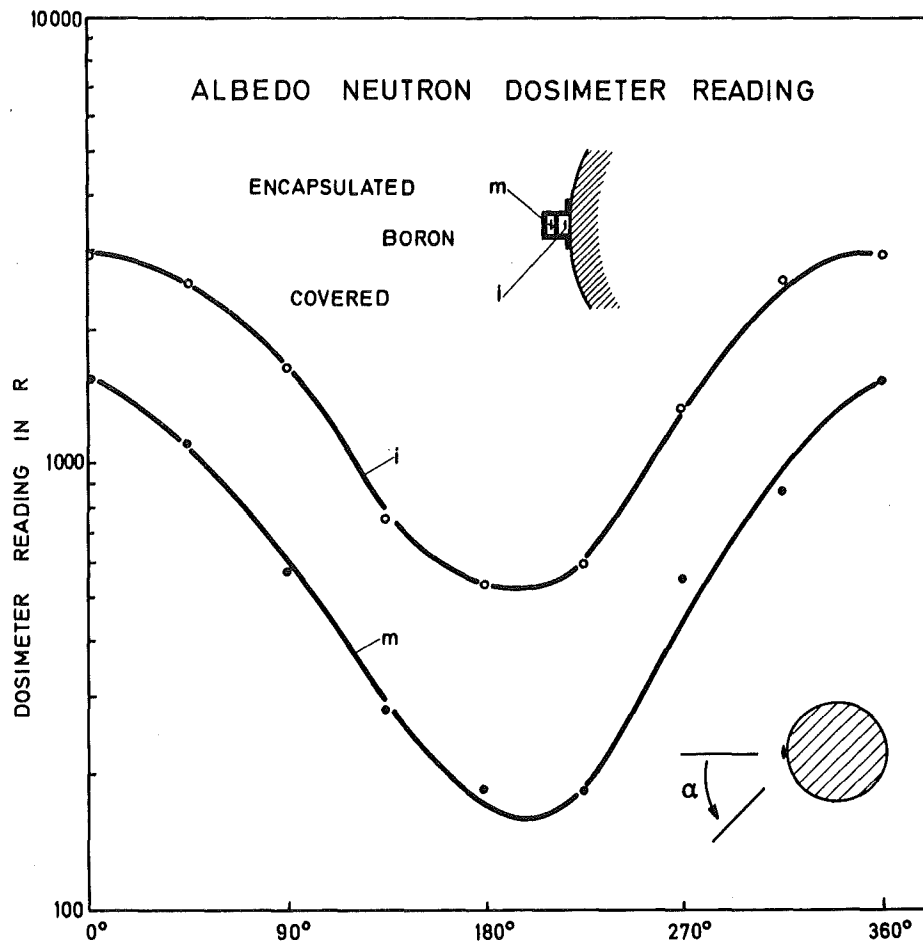


Fig. 7

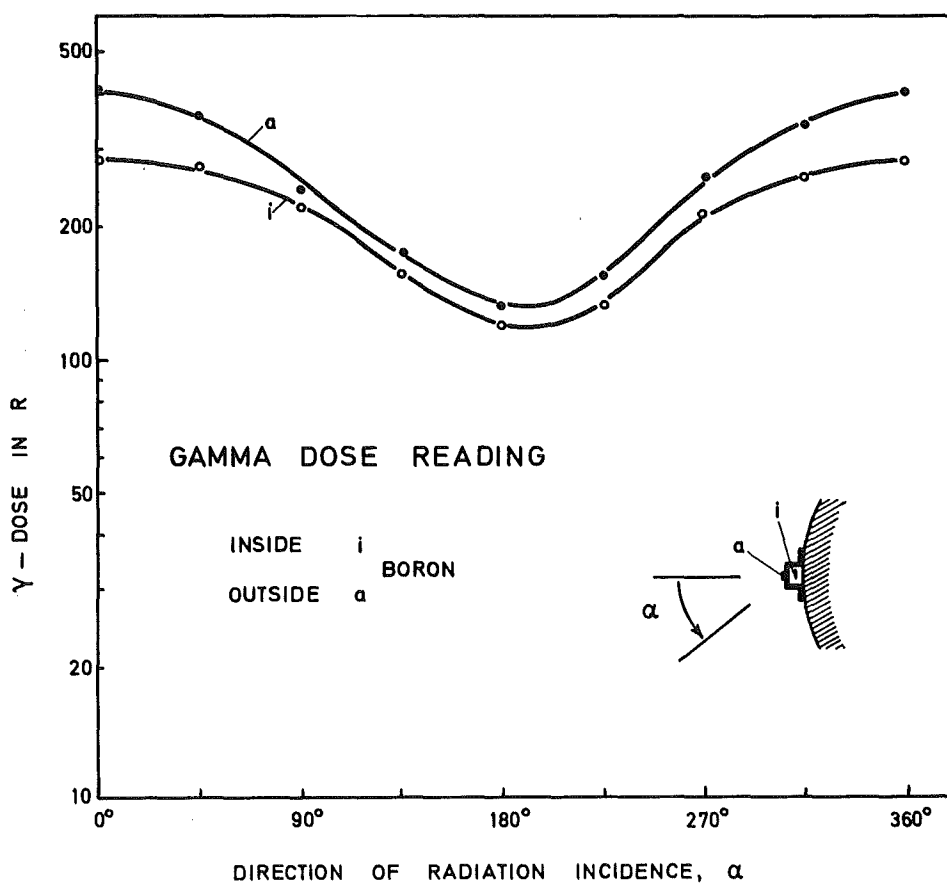


Fig. 8

#### 6.4 Phantom Studies with Neutron Detectors

The dependence of the detector sensitivity on the direction of neutron incidence was studied for the phantom irradiations with the neutron detectors used in the experiment. The directional response of the  $^{232}\text{Th}$  fission fragment track detector and of the gold foillis presented in Tab. 20 and the results of activation detectors are shown in Fig. 9 for an exposure on the bottle phantom 4 from Run No. 1. The lowest directional dependence was found for epithermal neutrons, the highest for thermal neutrons. The detector reading at  $180^\circ$  is 10 % for fast neutrons and 21 % for epithermal neutrons.

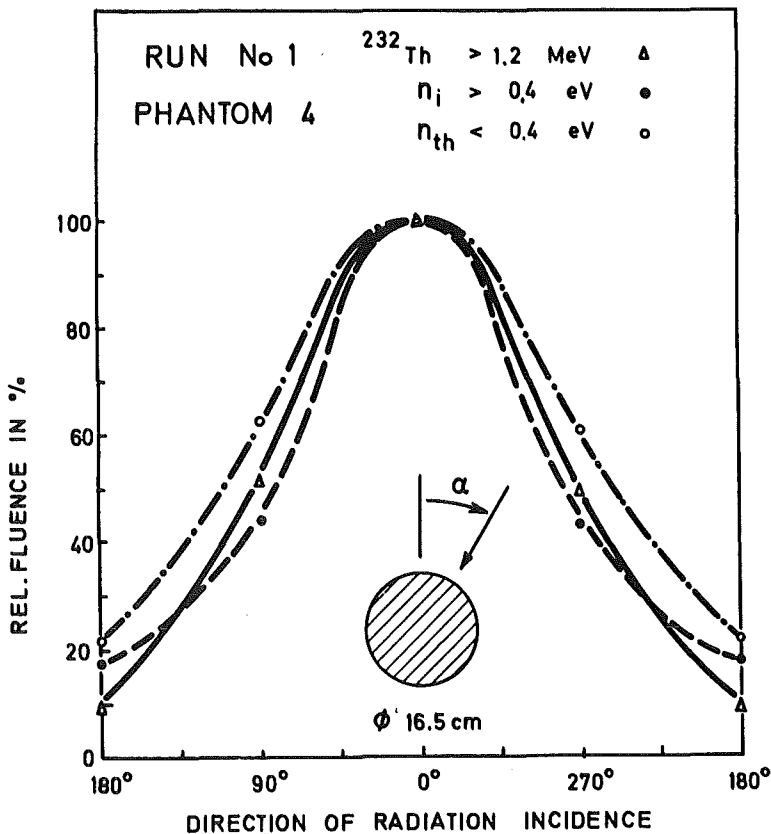


Fig. 9: Directional dependence of the neutron fluence

Fig. 7: Directional dependence of the neutron dose reading of the albedo dosimeter

Fig. 8: Directional dependence of the gamma dose reading of the albedo dosimeter

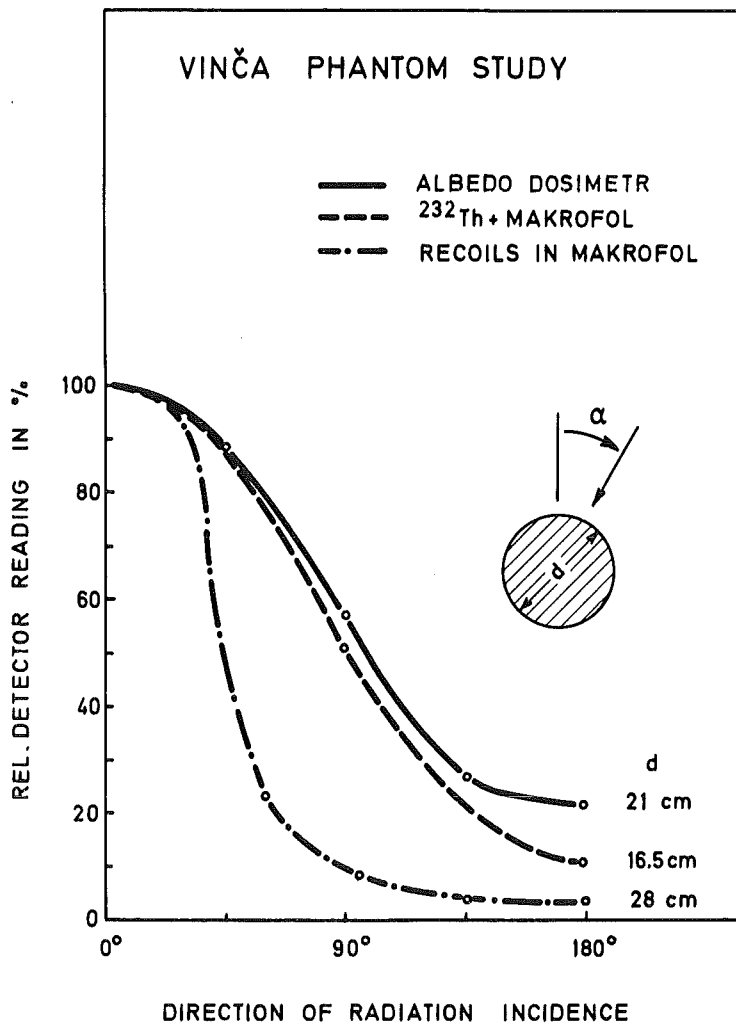
Table 20: Directional Dependence of Fluence Results for the Bottle Phantom Stations

NEUTRON FLUENCE IN $10^{10}$ n/cm <sup>2</sup>												
	Au < 0.4 eV				Au > 0.4 eV				<sup>232</sup> Th > 1.2 MeV			
	0°	90°	270°	180°	0°	90°	270°	180°	0°	90°	270°	180°
<u>RUN 1</u>												
Phantom 1	5.05	3.17	1.91	0.97	2.78	1.15	1.24	0.385	0.126	0.123	0.103	0.012
Phantom 2	4.95	2.61	3.5	1.02	2.56	0.96	1.38	0.425	0.186	0.127	0.123	0.022
Phantom 3	4.82	3.03	2.94	1.06	2.4	1.06	1.03	0.42	0.196	0.101	0.097	0.019
Phantom 4	4.45	1.49	3.50	1.07	2.56	1.01	2.0	0.46	0.163	0.092	0.156	0.036
<u>RUN 2</u>												
Phantom 1	34.8	17.6	-	5.8	16.6	7.7	-	2.3	0.86	0.91	0.82	0.10
Phantom 2	33.8	13.9	16.9	6.2	16.5	7.9	4.9	2.2	1.06	0.74	0.51	0.11
Phantom 3	33.8	16.8	14.9	6.8	17.2	6.8	7.8	2.4	1.02	0.246	0.63	0.10
Phantom 4	27.8	15.3	21.5	7.8	14.6	6.4	10.5	2.9	0.92	0.61	0.93	0.2

Table 21: Dose Estimates and Albedo Dosimeter response for the Bottle Phantom Stations

	NEUTRON DOSE			ALBEDO DOSIMETER READING					
	h <sub>erg</sub> ·g <sup>-1</sup>	rd	rem	R·h <sub>erg</sub> <sup>-1</sup> ·g		R·rd <sup>-1</sup>		R·rem <sup>-1</sup>	
<u>RUN 1</u>									
Phantom 1	13.3	18.9	175.5	12.5	15.4	8.8	10.8	0.95	1.16
Phantom 2	15.3	21.1	197.4	13.6	16.7	9.8	12.1	1.05	1.3
Phantom 3	15.4	21.1	197.3	13.2	17	9.7	19.0	1.04	1.33
Phantom 4	14.3	19.7	182.4	11.9	29.7	8.7	21.5	0.94	2.35
				12.3	19.7	9.3	14.4	1.0	1.54
<u>RUN 2</u>									
Phantom 1	92.9	130	1226	15.8	20.7	11.3	14.8	1.2	1.57
Phantom 2	88.4	125	1172	12	17.1	8.5	12.1	0.91	1.29
				14.7	20	10.4	14.1	1.2	1.11
Phantom 3	97.6	136	1270	13.3	23	9.6	16.5	1.02	1.76
Phantom 4	88.8	122	1136	13.5	20	9.9	14.5	1.06	1.56
				13.8	20	10	14.3	1.08	1.46

A plastic belt of Makrofol E was used as a recoil track detector to determine the direction of the neutron incidence. Such a belt consists of a 5 cm wide Makrofol strip welded into a thinner foil. After exposure on the bottle-phantom discs of 1 cm diam. Were punched out of the belt at equal distances, etched and counted microscopically. In Fig. 10 the relative number of recoil and  $(n,\alpha)$  tracks is presented as a function of the detector position with respect to the direction of the radiation incidence. The decrease of the track number for angles between  $45^\circ$  and  $90^\circ$  is mainly due to the directional dependence of the detector response and the low-energy cutoff of 1 MeV for the recoil track detection. A free air exposure parallel to the foil surface yields only 40 % of the tracks [4].



Tab. 11: Directional dependence of the albedo neutron dosimeter, of the  $^{232}\text{Th}$  fission fragment detector and of the Makrofol recoil track detector found for the Vinča neutron spectrum on the surface of bottle phantoms of various diameters

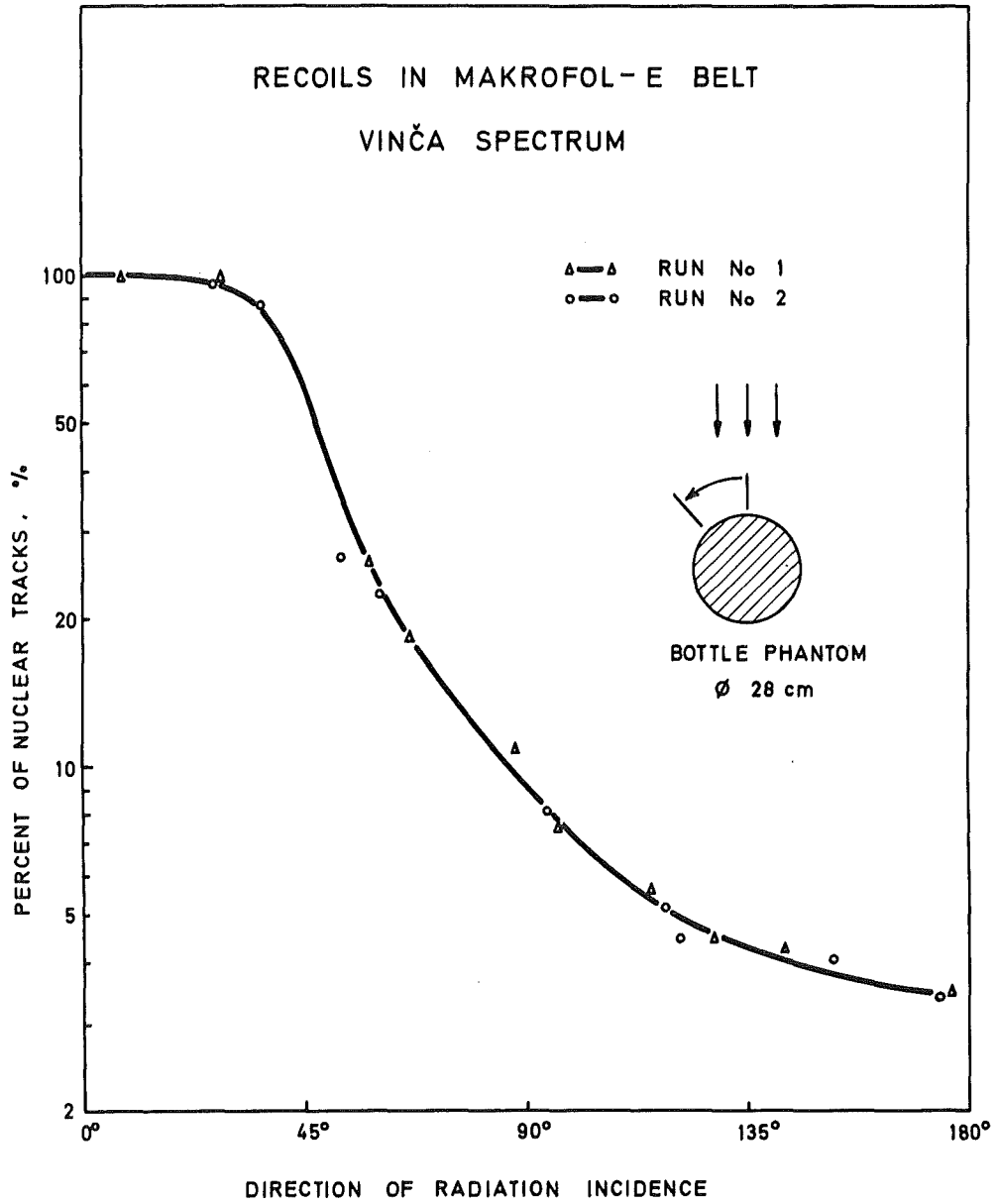
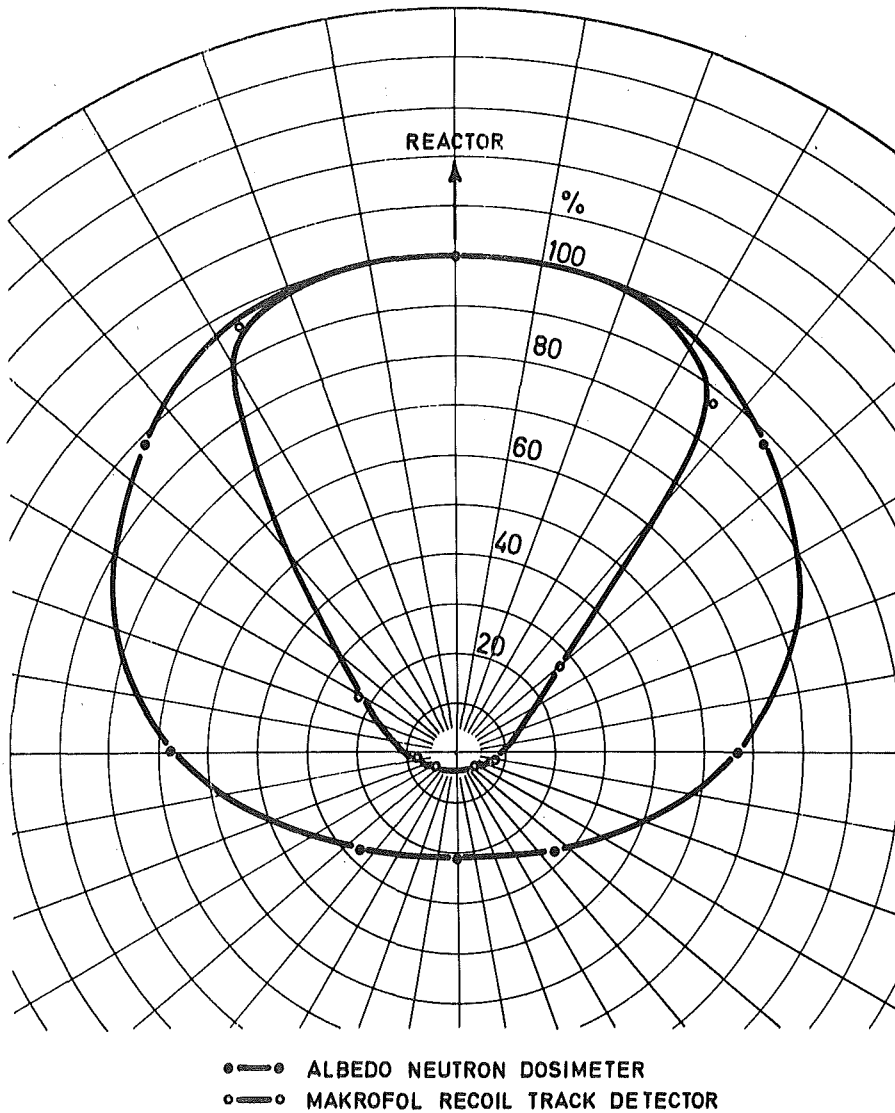


Fig. 10: The relative number of recoil tracks measured with a Makrofol E belt on the surface of a bottle phantom as a function of the direction to the radiation incidence for the Vinča neutron spectrum

The directional response of neutron detectors exposed on the phantom is influenced by neutron absorption, backscattering and change of the neutron energy distribution due to moderation in the phantom. The decrease of the detector reading extremely depends on the different threshold energies of the detectors and on the moderation of the fission spectrum, the lower energies of which are cut off to different extent. This detector characteristics are shown in Fig. 11, where the relative detector reading of the albedo dosimeter, of the  $^{232}\text{Th}$  threshold detector and the Makrofol recoil track detector is plotted against the direction of the neutron incidence for bottle phantom exposures at the Vinča reactor. The directional dependence at the bottle phantom was found to be 57 %, 51 % and 9 % at  $90^\circ$ , and 21 %, 11 % and 4 % at  $180^\circ$  for the albedo dosimeter, the  $^{232}\text{Th}$  fission detector and the Makrofol recoil detector respectively. Not only the cut off of the lower energy by the threshold but also the size and dimension of the phantom changes the detector sensitivity, especially for a radiation incident at  $180^\circ$ . The Makrofol recoil track detector has shown a similar directional dependence at the steel moderated spectrum of the HPRR in Oak Ridge [2], for the Bomab phantom which has a cylindrical cross section.

It is shown in Fig. 12 that an albedo dosimeter does not underestimate the neutron dose more than other neutron detectors. Using an albedo dosimeter system consisting of one dosimeter on each side of the body, the directional dependence can be reduced to 20 % [5]. The use of an Makrofol belt offers the opportunity to measure the dose around the body surface as well as to find out the direction of the radiation incidence. The energy cut off depends, however, on the neutron spectrum and therefore also on the direction of the radiation incidence. For a neutron dose estimation the directional response of the detector exposed free in the air has to be considered and taken into account.



DIRECTIONAL DEPENDENCE AT THE VINČA REACTOR

Fig. 12: Directional dependence of the albedo neutron dosimeter and the Makrofol recoil track detector at the Vinča reactor

Acknowledgements

The authors wish to thank Dr. I. Miric and the staff of the Boris Kidrič Institute for the kind hospitality and help during the intercomparison experiment

References

- [1] E. Piesch: Report KFK-1462, 1971
- [2] E. Piesch: Report KFK-1630, 1972
- [3] E. Piesch: Proc. IAEA-Symp. Neutron Monitoring,  
p. 471, 1967
- [4] E. Piesch: Proc. IAEA Symp. New Rad. Detectors,  
p. 399, 1971
- [5] E. Piesch, B. Burgkhardt: Proc. IAEA Symp.  
Neutron Monitoring Vol. II, p.31, 1973
- [6] E. Piesch: Developments in Radiophotoluminescence  
Dosimetry in Attix: Topics in Rad.  
Dosimetry, Academic press, p. 461-532, 1972
- [7] N. Adams, J.A. Dennis: Report AERE-R 6008, 1969
- [8] D.R. Stone et al: Health Physics 18, 69, 1970
- [9] F.F. Haywood: Report ORNL-TM-3551 NAD Appendix IX, 1972
- [10] J.A. Auxier, W.S. Snyder and T.D. Jones:  
in F.H. Attix and W.C. Roesch  
Radiation Dosimetry Vol. 1, p. 275,  
Academic Press
- [11] N. Brica, Nguyen van Dat, L. Prtheoes:  
Rapport CEA R-4226-1971
- [12] N. Brica: private communication
- [13] E. Piesch, B. Burgkhardt: to be published
- [14] E. Piesch, B. Burgkhardt: paper presented at IRPA-Congress  
Washington, Sept. 1973, to be published
- [15] E. Piesch, B. Burgkhardt: to be published